A Comparison Study the Effect of Doping by Ga_2O_3 and CeO_2 On the Structural and Optical Properties of SnO_2 Thin Films

Maab A. Abood*, Bushra A. Hasan

Department of physics, collage of science, University of Baghdad, Baghdad, Iraq

Abstract:

   This research deals with the effect of gallium oxide and cerium oxide as dopants on the structural and optical characteristics of tin oxide. Gallium and cerium oxide doped tin oxide was prepared with different doping concentrations (0, 0.03, 0.05 and 0.07) wt. pure and doped tin oxide thin films were prepared by the pulsed laser deposition technique. X-ray diffraction and UV-Visible spectrophotometer were employed to investigate both oxides doping effects. Results showed that all prepared samples have poly-crystalline structure with a preferred plane of crystal growth along (110), where the crystal size grew from 40.3 nm to 64.5 nm and to 43.5 nm for Ga_2O_3 and CeO_2 doped tin oxide thin films, respectively. Transmittance decreased drastically by increasing the doping ratio of gallium oxide. In contrast, it increased by increasing the doping ratio of cerium oxide. The optical energy gap was found to change in nonsystematic sequence with the increase of Ga_2O_3 doping concentration, while it decreased monotonically by increasing the CeO_2 doping concentration.

Keywords: tin oxide, gallium oxide, cerium oxide, x-ray diffraction, optical energy gap

دراسة مقارنة تأثير التطعيم بأوكسيد الكاليوم واوكسيد السيريوم على الخواص التركيبية والبصرية لاغشية اوكسيد القصدير الرقيقة

مآب عبدالسلام عبود*, بشرى عباس حسن

قسم الفيزياء , كلية العلوم, جامعة بغداد, بغداد, العراق

الخلاصة

   هذا البحث يهتم بعمل مقارنة بين تاثير ذرات التشويب من اوكسيد الكاليوم واوكسيد السيريوم على التركيب والخصائص البصرية لاغشية اوكسيد القصدير .في البدء تم تحضير مركبات من اوكسيد القصدير المطعم باوكسيد الكاليوم واوكسيد السيريوم بتراكيز مختلفة(0, 0.03, 0.05 and 0.07)wt. تم تحضير اغشية رقيقة من التراكيز السبع باستخدام تقنية الترسيب بالليزر النبضي. استخدمت تقنيات حيود الاشعة السينية والمطياف البصري لاستقصاء تأثير هذين الاوكسيدين .اظهرت النتائج ان جميع النماذج المحضرة كانت متعددة البلورات ولها مستوي مفضل للنمو عند(110) حيث يزداد حجم البلورة من 40.3 nm الى 64.5 nm والى 43.5 nm لأغشية اوكسيد القصدير المطعمة بأوكسيد الكاليوم والسيريوم على التوالي لقد وجد ان النفاذية

_____

*Email: returne.salam@gmail.com

<div dir="rtl">

تقل وبحدة مع زيادة نسبة التطعيم بأوكسيد الكاليوم بينما يتضح ان النفاذية ي تزداد مع نسبة التطعيم بأوكسيد

السيريوم   . لقد وجد ان فجوة الطاقة البصرية تتغير بصورة غير منتظمة مع زيادة نسبة التطعيم باوكسيد

الكاليوم بينما وجد انها تقل وباضطراد مع زيادة نسبة التطعيم باوكسيد السيريوم.

</div>

1. Introduction

Many researchers have great interest in the fabrication of tin oxide-based films as transparent conductors due to their possible applications in optoelectronic devices, smart sensors and green energy devices [1,2]. Tin oxide (SnO_2) is an n-type semiconductor in nature; it is with rutile structure (a=b=5.0 A, c=3.187 A) [3,4] and has a direct energy band gap of 3.60–4eV. It is widely utilized in gas sensors, photo-detectors [5], solar cells [6], light emitting diodes [7], and transistors [8]. Group-III elements such as Ga, Al, In, and so on represent the most common dopant elements; they play the role of effective donors [9]. Singh et al. have discovered that the incorporation of group III elements on the Sn site in SnO_2 lattice creates shallow acceptors resulting in excellent solubility [10]. From theoretical studies, Ga has been predicted as one of the good sources of the p-type dopant [11]. SnO_2 was utilized as a photo-catalyst for the degradation of different environmental contaminant materials like phenols, dyes, etc. [12,13]. Nonetheless, the SnO_2 suffers from low photo-catalytic efficiency due to its high recombination rate of the photo-generated electron–hole pairs [14]. It is greatly significant to promote SnO_2 photo-catalytic performance. Important efforts were advanced for boosting SnO_2 photo-catalytic activity. For the purpose of endowing SnO_2 with a higher photo-catalytic efficiency and increasing its competitiveness, SnO_2 has been doped with different oxides such as cerium oxide (CeO_2) and gallium oxide (Ga_2O_3).

Cerium (Ce) has attracted the attention as a dopant among a number of metal oxides, like TiO_2 [16], ZnO and SnO_2, as a result of its important characteristics that arise from shell 4f electron availability [15]. Doped and undoped SnO_2 have been successfully synthesized using a variety of experimental approaches[17], like the sol-gel [18], electrospinning, radio frequency sputtering [19, 20] that result in obtaining crystallites of different sizes and morphologies. In the literature, several studies have focused on the practical applications and characteristics of SnO_2. The benefits that SnO_2 offers make it one of the possible rivals for the two common semiconductors TiO_2 and ZnO in the photocatalysis domain

The present work shed light on the effect of two different dopant oxides: gallium oxide (Ga_2O_3) and cerium oxide (CeO_2) on the optical and structural characteristics of tin oxide. CeO_2 and Ga_2O_3-doped SnO_2 thin film samples, were deposited on glass substrates by the pulsed laser deposition (PLD)technique.

2. Experimental

In this work, SnO_2, Ga_2O_3 and CeO_2 oxides with high purity (three nines after digit) were supplied from Aldrich. Different compounds with various doping ratios according to the atomic weight. They were weighted using an electronic balance with four numbers after the point (10^{-4} gm). The mixtures of the two types of compounds named tin oxide doped with gallium oxide and cerium oxide with different ratio (0, 3%, 5% and 7%) were put in a quartz ampoule with a length ~ 25cm and internal diameter of~ 8mm, evacuated to ~10^{-3} Torr and heated in an oven at 1273 K for one hour and then were left to cool at room temperature. Then the obtained materials were grinded and pressed to pellets shape of 1 cm diameter and 0.5 cm thickness. Two types of samples of SnO_2:Ga_3O_4 and SnO_2:CeO_2 with various doping ratios (0, 0.03, 0.05, and 0.07) were prepared using the PLD method. The deposition was done

in vacuum of 2×10^{-2} Torr using Nd:YAG laser beam (with energy, pulsed and frequency of 400 mJ, 200 and 6Hz, respectively). The laser beam was focused through a window on the target. The ablated atoms incident on the glass substrates created the thin films. The film thickness (t) is given by:

$$t = \frac{\lambda}{2}\frac{\Delta x}{x} \qquad (1)$$

Where: Δx, x and λ are the shift between interference fringes, the distance between the interference fringes and the wavelength of He:Ne (632.8 nm), respectively. The crystal structure and crystallinity of Ga_2O_3 doped and CeO_2 doped TiO_2 thin films were determined by the XRD with CuKα radiation (λ= 1.5406Å), and grazing incidence angle of 0.80^{o}. The optical measurements were made using a UV-Visible spectrophotometer (Shimadzu UV-1800. Made in Japan).The wavelengths of the device(190-1100nm)were used to determine both the absorbance and the transmittance spectra of the prepared (SnO_2): (Ga_2O_3,CeO_2) thin films. The following equation:

$$\alpha = 2.303A/t \qquad (2)$$

was used to calculate the absorption coefficient, where A represents absorbance and t is the thin film thickness. The optical energy gap was estimated with the use of Tauc relation for direct permitted transitions [21]:

$(\alpha h\nu) = B(h\nu - E_g)^{r}$ (3)

Where: B represents a constant and E is the optical band gap. The equations used to measure the optical constants, including refractive index, extinction coefficient, real and imaginary parts of the dielectric constants are

$$n = (4R/(R-1)^2 - k^2)^{1/2} - (R+1)/(R-1) \qquad (4)$$
$$R = (n-1)^2 + k^2/(n+1)^2 + k^2 \qquad (5)$$
$$\varepsilon_r = n^2 - k^2 \qquad (6)$$
$$\varepsilon_i = 2nk \qquad (7)$$

In that order transmittance and absorption tests were carried out.

3. Result and discussion

3.1 Structural properties

3.1.1 Structural analysis of (SnO_2):(Ga_2O_3) thin films

Figure 1 depicts the XRD patterns of pure SnO_2 and Ga_2O_3 doped SnO_2(of different doping ratios, 3%-7%) thin films. Five diffraction peaks were identified as (110) (101) (200) (211) and (301) reflections of the tetragonal structure (as shown in Table (1)) .
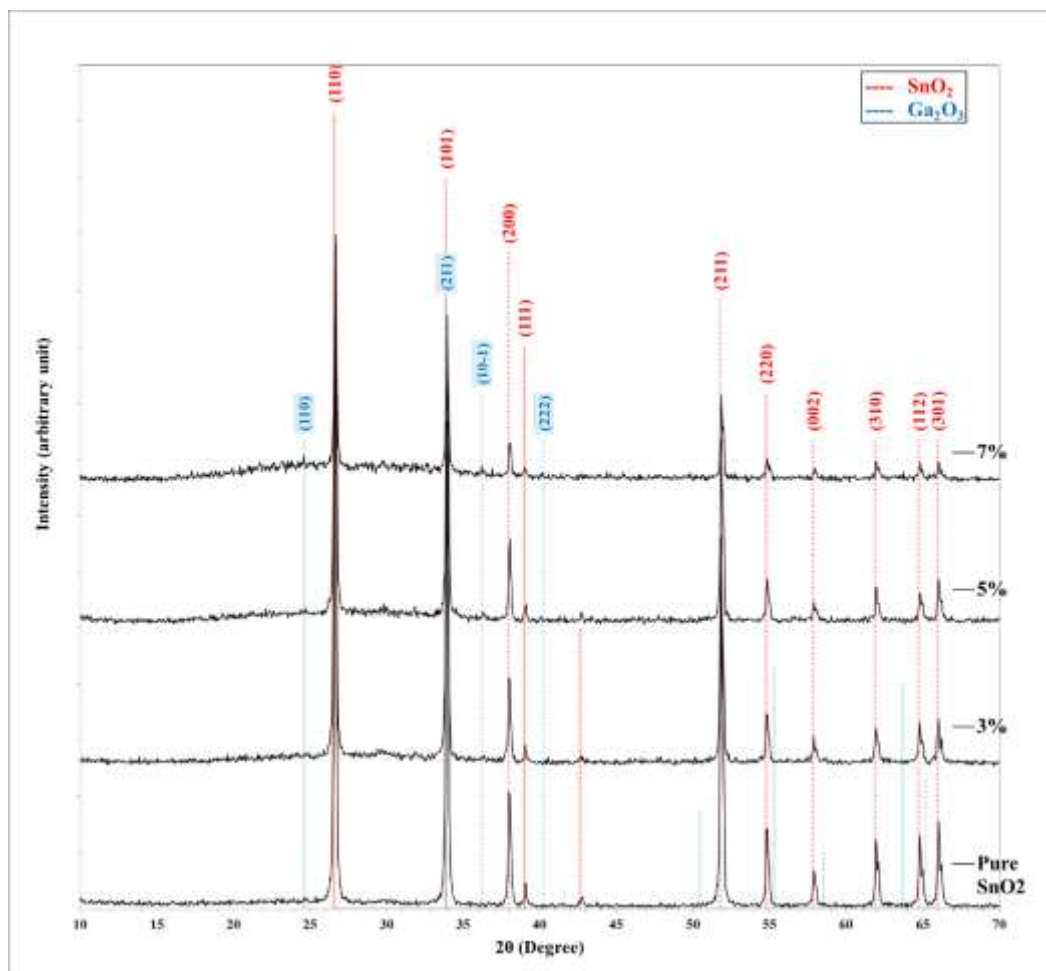
Figure 1: XRD patterns for the pure SnO_2 and Ga_2O_3 doped SnO_2 thin films

The peaks corresponding to the SnO_2 are declared for all samples while the peaks corresponding to Ga_2O_3 doped SnO_2 samples referred that crystallization take place and the formation of a mixed oxide and well defined mixing of tin and gallium phases is observed [22].

Table 1: X-ray diffraction obtained data of $(SnO_2):(Ga_2O_3)$thin films.

x	2θ (Deg.)	FWHM (Deg.)	d_{hkl} Exp.(Å)	C.S (nm)	hkl	Phase
	26.67	0.2026	3.3404	40.3	(110)	SnO_2
	33.96	0.2279	2.6377	36.5	(101)	SnO_2
	38.04	0.2280	2.3638	36.9	(200)	SnO_2
	39.05	0.2026	2.3048	41.6	(111)	SnO_2
Pure	51.87	0.2786	1.7614	31.7	(211)	SnO_2
	54.83	0.2786	1.6730	32.1	(220)	SnO_2
	57.92	0.3040	1.5909	29.9	(002)	SnO_2
	61.97	0.3039	1.4962	30.5	(310)	SnO_2
	64.81	0.2786	1.4374	33.8	(112)	SnO_2
	66.05	0.2786	1.4134	34.0	(301)	SnO_2

	26.67	0.1772	3.3404	46.1	(110)	SnO_2
	33.96	0.2026	2.6377	41.0	(101)	SnO_2
	38.01	0.2027	2.3653	41.5	(200)	SnO_2
	39.08	0.2279	2.3033	37.0	(111)	SnO_2
3%	51.87	0.2786	1.7614	31.7	(211)	SnO_2
	54.85	0.3040	1.6723	29.5	(220)	SnO_2
	57.92	0.2786	1.5909	32.6	(002)	SnO_2
	61.97	0.3039	1.4962	30.5	(310)	SnO_2
	64.81	0.2533	1.4374	37.2	(112)	SnO_2
	66.02	0.2532	1.4139	37.4	(301)	SnO_2
	26.69	0.1726	3.3372	47.3	(110)	SnO_2
	33.96	0.2026	2.6377	41.0	(101)	SnO_2
	36.34	0.3039	2.4702	27.5	(10-1)	Ge_2O_3
	38.06	0.2533	2.3623	33.2	(200)	SnO_2
	39.10	0.2786	2.3019	30.3	(111)	SnO_2
5%	51.87	0.2786	1.7614	31.7	(211)	SnO_2
	54.85	0.2786	1.6723	32.1	(220)	SnO_2
	57.92	0.2786	1.5909	32.6	(002)	SnO_2
	62.00	0.2786	1.4957	33.3	(310)	SnO_2
	64.86	0.2786	1.4364	33.8	(112)	SnO_2
	66.05	0.2786	1.4134	34.0	(301)	SnO_2
	24.61	0.1266	3.6139	64.3	(110)	Ge_2O_3
	26.67	0.1266	3.3404	64.5	(110)	SnO_2
	33.96	0.1773	2.6377	46.9	(101)	SnO_2
	36.21	0.2026	2.4785	41.3	(10-1)	Ge_2O_3
	38.06	0.2532	2.3623	33.2	(200)	SnO_2
7%	39.02	0.2533	2.3062	33.3	(111)	SnO_2
	51.87	0.2533	1.7614	34.9	(211)	SnO_2
	54.85	0.2533	1.6723	35.3	(220)	SnO_2
	57.94	0.2532	1.5903	35.9	(002)	SnO_2
	62.00	0.2533	1.4957	36.6	(310)	SnO_2
	64.83	0.2533	1.4369	37.2	(112)	SnO_2
	66.02	0.2532	1.4139	37.4	(301)	SnO_2

3.1.2 Structural analysis of SnO_2:CeO_2 thin films

The XRD patterns of pure SnO_2 and CeO_2 doped SnO_2 thin films are illustrated in Figure 2. XRD pattern of the pure SnO_2 shows distinctive peaks at 2θ of 26.67^o, 33.95^o, 37.95^o, 38.97^o, 51.75^o, 54.76^o, and 65.96^o, corresponding to (110), (101), (200), (211), (220), (112), and (310) planes of SnO_2 (as shown in Table(2)). This data coincided with the JCPDS data [23 -25].

The synthesized thin films crystalline structure were tetragonal rutile based upon JCPDS reference data. CeO_2 doped SnO_2 XRD patterns appear quite similar to that of the pure SnO_2 with the SnO_2 crystalline structure [26].
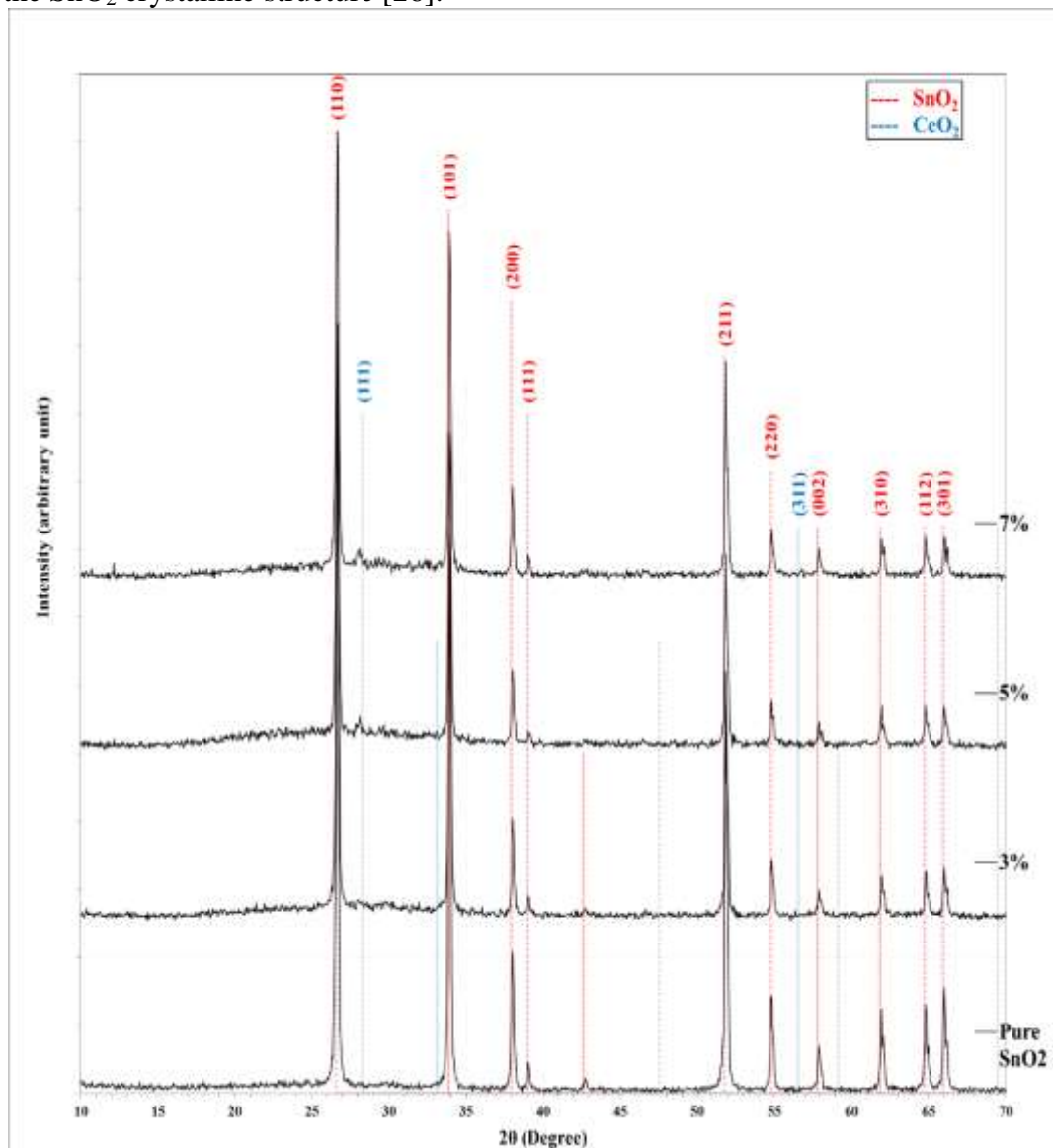
Figure 2: XRD patterns of the pure SnO_2 and CeO_2 doped SnO_2 thin films

Table 2: The XRD obtained data of SnO_2:CeO_2 thin films.

x	2 θ (Deg.)	FWHM (Deg.)	d_{hkl} Exp.(Å)	CS (nm)	hkl	Phases
	26.67	0.2026	3.3404	40.3	(110)	SnO_2
	33.96	0.2279	2.6377	36.5	(101)	SnO_2
	38.04	0.2280	2.3638	36.9	(200)	SnO_2
	39.05	0.2026	2.3048	41.6	(111)	SnO_2
Pure	51.87	0.2786	1.7614	31.7	(211)	SnO_2
	54.83	0.2786	1.6730	32.1	(220)	SnO_2
	57.92	0.3040	1.5909	29.9	(002)	SnO_2
	61.97	0.3039	1.4962	30.5	(310)	SnO_2

	64.81	0.2786	1.4374	33.8	(112)	SnO_2
	66.05	0.2786	1.4134	34.0	(301)	SnO_2
	26.65	0.2015	3.3422	40.5	(110)	SnO_2
	33.95	0.2015	2.6381	41.2	(101)	SnO_2
	38.04	0.2267	2.3639	37.1	(200)	SnO_2
	39.07	0.1763	2.3038	47.8	(111)	SnO_2
3%	51.84	0.2519	1.7623	35.1	(211)	SnO_2
	54.84	0.2771	1.6728	32.3	(220)	SnO_2
	57.88	0.2770	1.5918	32.8	(002)	SnO_2
	61.96	0.2770	1.4964	33.5	(310)	SnO_2
	64.84	0.2771	1.4369	34.0	(112)	SnO_2
	66.07	0.2771	1.4130	34.2	(301)	SnO_2
	26.65	0.1900	3.3422	43.0	(110)	SnO_2
	28.11	0.3527	3.1718	23.2	(111)	CeO_2
	33.95	0.1763	2.6381	47.1	(101)	SnO_2
	38.04	0.2267	2.3639	37.1	(200)	SnO_2
	39.09	0.2267	2.3023	37.2	(111)	SnO_2
5%	51.84	0.2771	1.7623	31.9	(211)	SnO_2
	54.81	0.2519	1.6735	35.5	(220)	SnO_2
	57.88	0.2771	1.5918	32.8	(002)	SnO_2
	61.99	0.2519	1.4958	36.8	(310)	SnO_2
	64.79	0.2519	1.4379	37.4	(112)	SnO_2
	66.07	0.3274	1.4130	29.0	(301)	SnO_2
	26.70	0.1880	3.3361	43.5	(110)	SnO_2
	28.09	0.3779	3.1746	21.7	(111)	CeO_2
	33.95	0.2015	2.6381	41.2	(101)	SnO_2
	38.04	0.2267	2.3639	37.1	(200)	SnO_2
7%	39.04	0.2267	2.3052	37.2	(111)	SnO_2
	51.84	0.2771	1.7623	31.9	(211)	SnO_2
	54.84	0.2267	1.6728	39.5	(220)	SnO_2
	56.78	0.2519	1.6202	35.9	(311)	CeO_2
	57.88	0.2015	1.5918	45.1	(002)	SnO_2
	61.94	0.2770	1.4969	33.5	(310)	SnO_2
	64.79	0.2771	1.4379	34.0	(112)	SnO_2
	66.07	0.2267	1.4130	41.8	(301)	SnO_2

3.2 Optical properties

3.2.1 *Optical characteristics of Ga_2O_3 doped SnO_2 thin films*

The optical transmission data(the absorption spectra) were obtained with a UV-Vis spectrophotometer. The transmittance spectra of Ga_2O_3 doped SnO_2 thin films were evaluated to investigate the optical characteristics, as depicted in Figure 3.

SnO_2 thin film has high transparency and average transmittance higher than 85% in the visible range. When Ga concentration was increased in the starting material, one can notice, besides variation of the film color (from transparent to brown), an average transmittance variation, approximately 65-75% for Ga_2O_3 doped SnO_2 films.
.
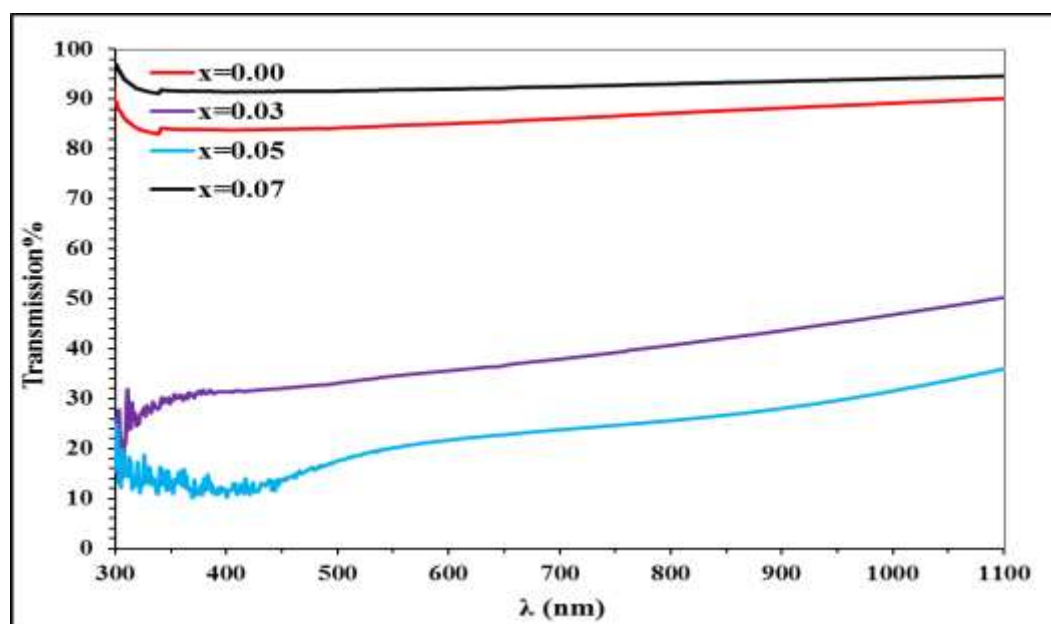
Figure 3: Transmittance spectra of the pure SnO_2 and Ga_2O_3 doped SnO_2 thin films.

As can be seen from Figure 4, the value of the direct band gap energy of pure SnO_2 thin film was 3.6eV. The values were 3.9, 2.8, and 3.5eV for the Ga_2O_3 doped SnO_2 thin films with doping concentrations of 0.03, 0.05, and 0.07, respectively. The maximal value of 3.9eV was obtained for the 3% Ga_2O_3 doped SnO_2. The energy gap values of tin oxide agree with that reported by Vincent[27] and Chopra et al. [29].

The variations of band gap depend on the effect of the free carrier electrons on the fundamental absorptions edge in near UV spectra [30]. The energy gap was found to change in a nonsystematic sequence i.e. increase and decrease; the decrease is attributed to the large crystallite size, which means that there are more atoms and also more atomic orbitals for overlap. Therefore, the number of molecular orbitals, bonding and antibonding, increases and the gap between the band gaps will decrease, and vice versa [31].
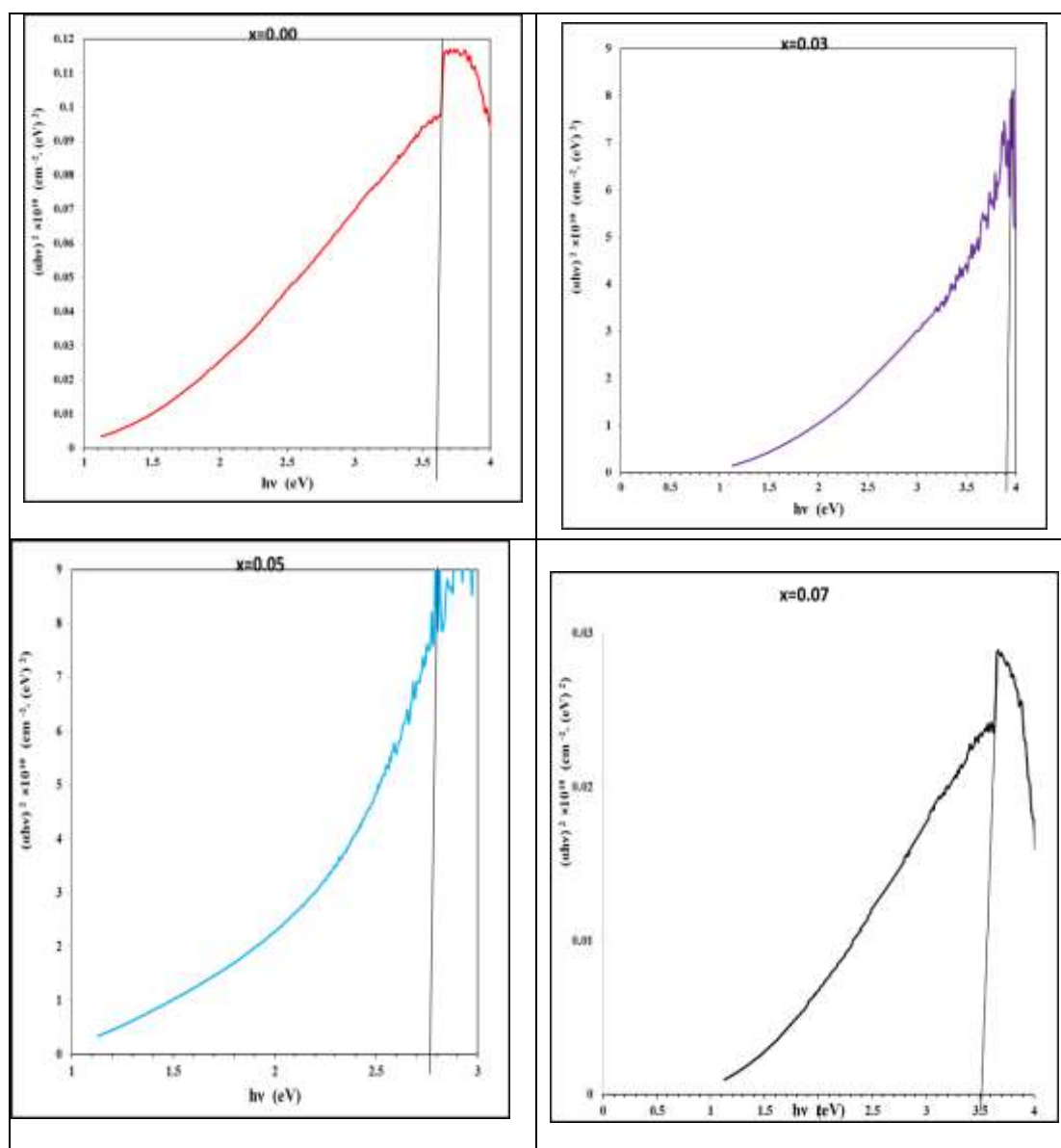
Figure 4: band gap of a pure SnO_2 and Ga_2O_3 doped SnO_2 thin films.

Figures 5 to 8 show plot diagrams of refractive index, extinction coefficient, refractive index, real and imaginary parts of the dielectric constant. It is clear that the addition of gallium oxide to tin oxide has changed the optical constant but in different manners depending on the added amount. The addition of gallium oxide, in general, reduced transmittance and hence all the optical constant values(n, k, ε_r, and ε_i). They increased with the increase of the doping concentration up till 5%, they decreased at (7%) doping concentration as shown in Table 3.
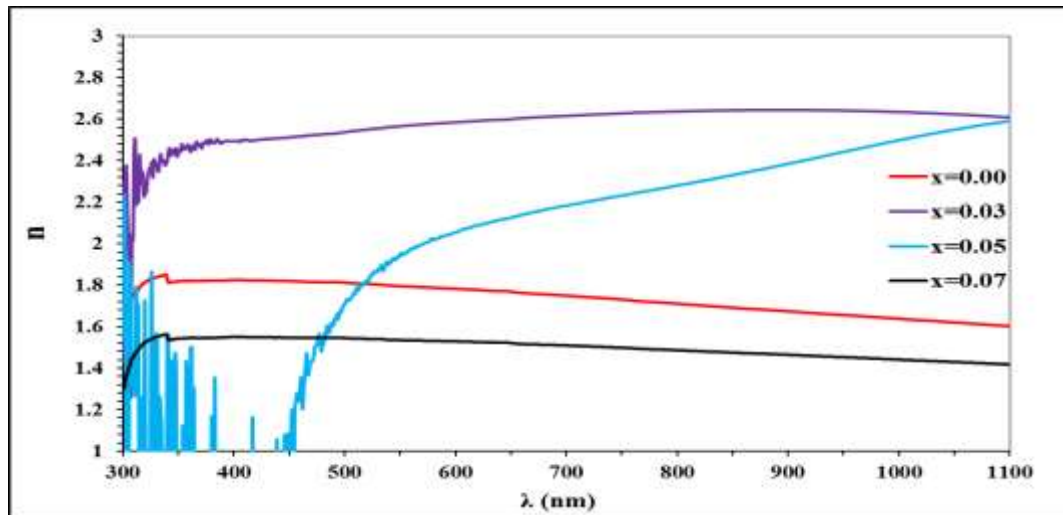
Figure 5: Refractive index as a function of wavelength for pure SnO_2 and Ga_2O_3 doped SnO_2 thin films.
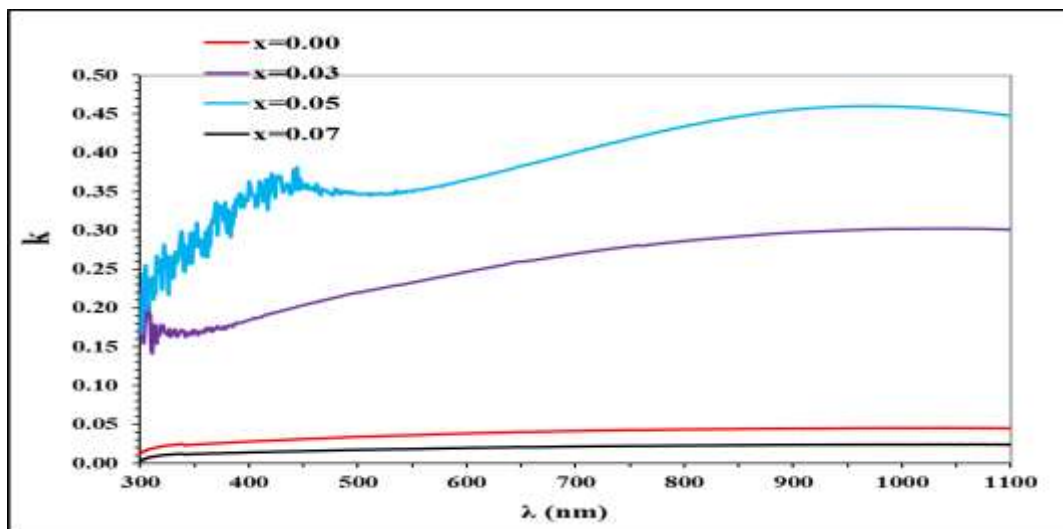
Figure 6: Extinction coefficient as a function of wavelength for pure SnO_2 and Ga_2O_3 doped SnO_2 thin films.
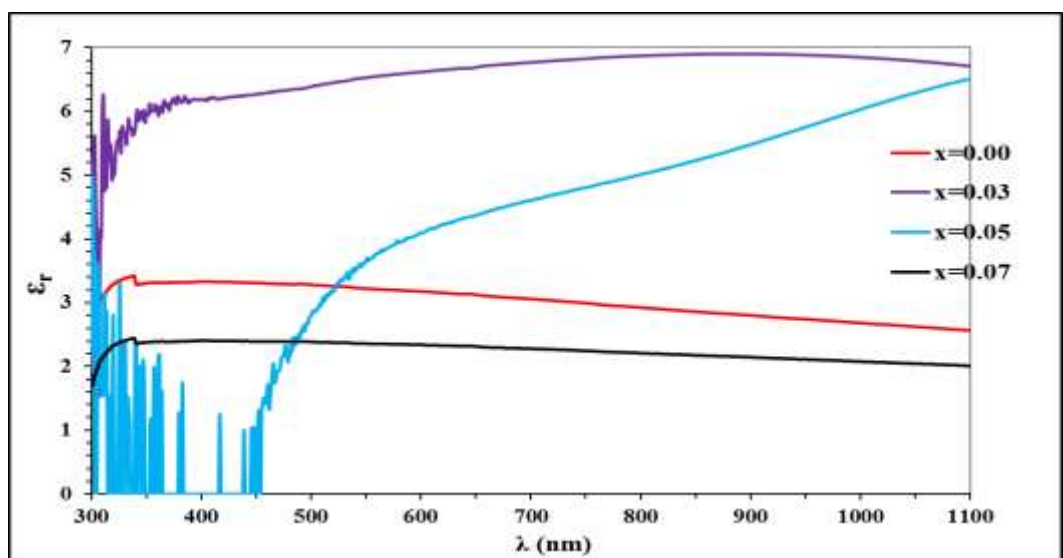
Figure 7: Real dielectric constant as a function of wavelength FOR pure SnO_2 and Ga_2O_3 doped SnO_2 thin films.
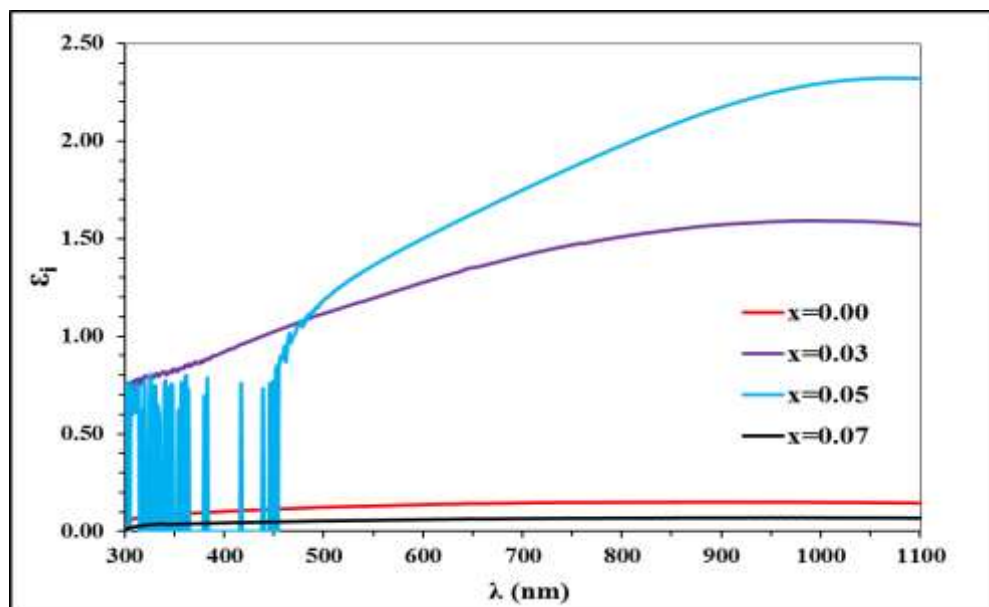
Figure 8: Imaginary dielectric constant as a function of wavelength for pure SnO_2 and Ga_2O_3 doped SnO_2 thin film

Table 3: transmittance, absorption coefficient, optical properties at $\lambda=550nm$ and optical energy gap of $SnO_2:Ga_2O_3$ thin film that have been prepared using the PLD technique

Samples	T%	α (cm^{-1})	k	n	ε_r	ε_i	Eg (eV)
SnO_2	84.7	8320	0.036	1.796	3.223	0.131	3.60
SnO_2:3%Ga_2O_3	34.51	53199	0.233	2.566	6.530	1.196	3.90
SnO_2:5%Ga_2O_3	20.09	80260	0.351	1.939	3.637	1.363	2.80
SnO_2:7%Ga_2O_3	91.3	4261	0.019	1.536	2.359	0.057	3.50

3-2-2 Optical properties of CeO$_2$ doped SnO$_2$ thin films

The optical transmittance spectra of pure and CeO$_2$-doped SnO$_2$ thin films were recorded in the wavelength range 300-1100nm. The spectra, Figure 9, showed that the prepared thin films are transparent in the visible range with a mean transmittance that ranges from 95 to 100%. The high level of the transparency has been observed for 5% CeO$_2$-doped SnO$_2$ film. Nonetheless, with the increase of doping level, film transmittance has decreased. It is well known that large surface roughness causes light diffusion and subsequently results in the reduction of transmittance. All the films presented a cut-off wavelength in the ultraviolet region at approximately 325nm. The band gap energies of the SnO$_2$ films were obtained from the transmittance spectra.
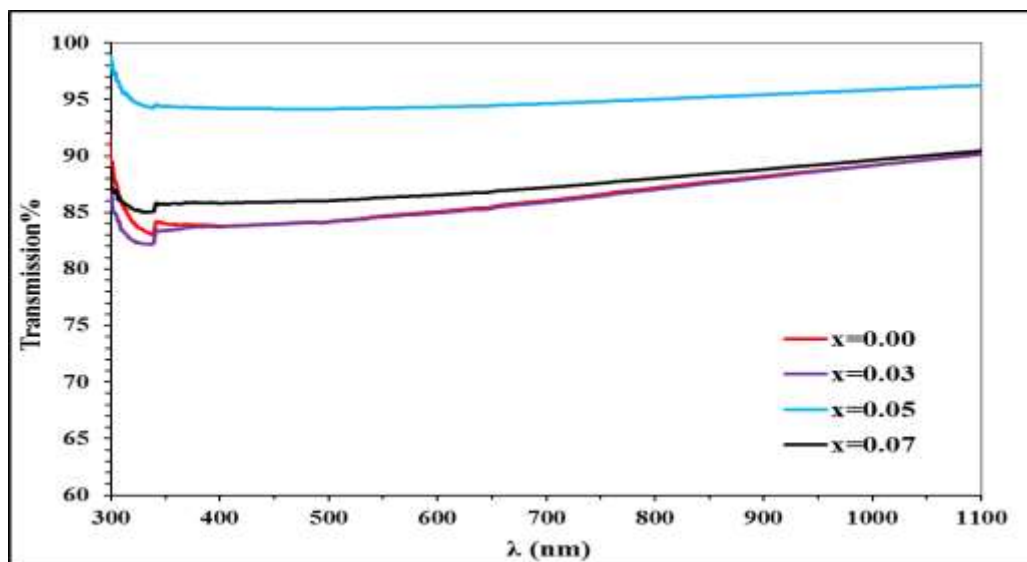
Figure 9: Transmission spectra for pure SnO_2 and CeO_2doped SnO_2
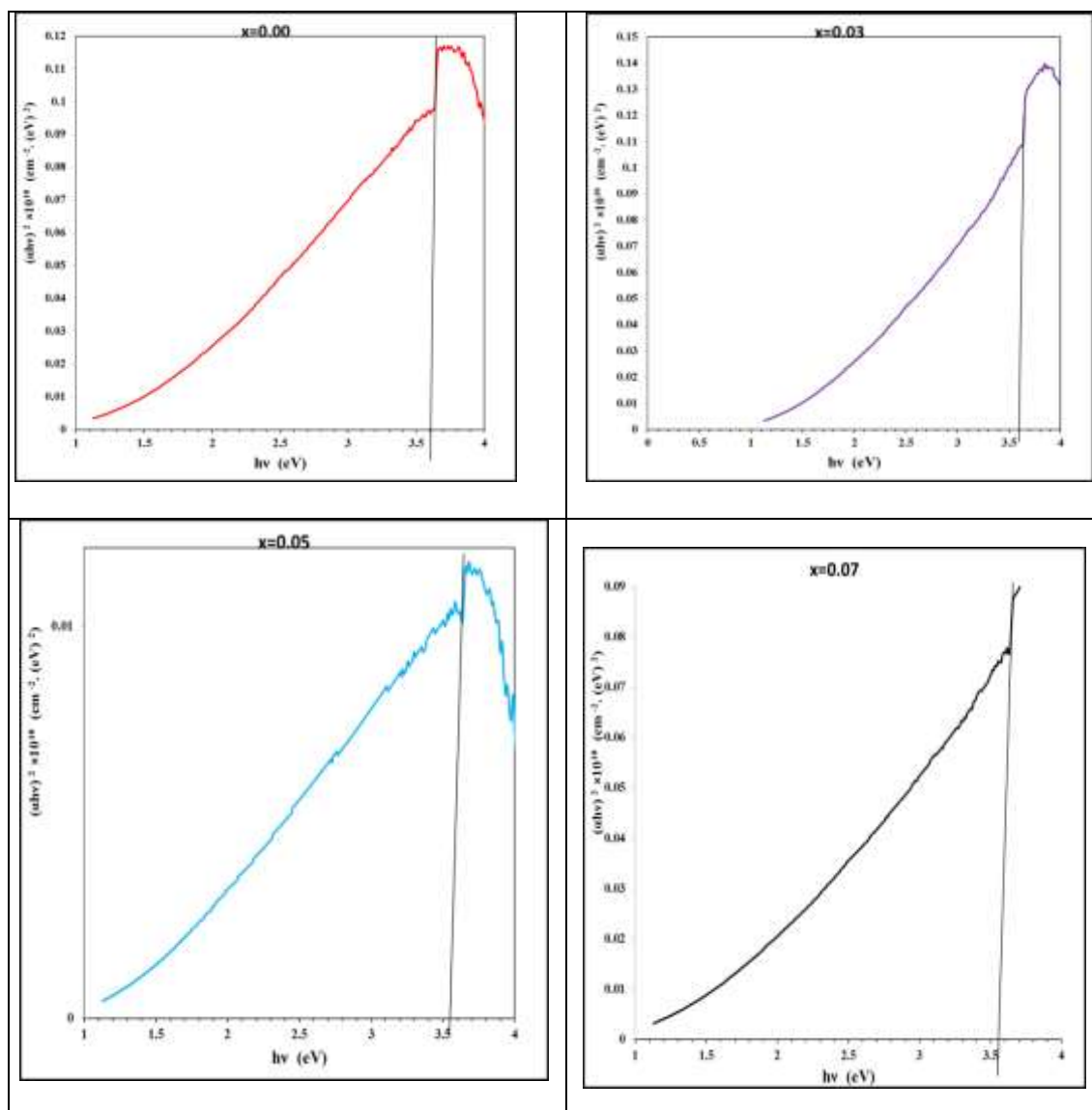
Figure 10: band gap for pure SnO_2 and CeO_2 doped SnO_2 thin films.

The energy values of the direct band gap are 3.65, 3.6, 3.58, and 3.55eV for the pure and CeO_2 doped SnO_2 of different doping concentrations thin films, as can be seen in Figure 10. The maximum value of 3.60 is obtained for pure SnO_2. It is obvious that band gap energy showed regular reduction by increasing the doping ratio. This behavior is ascribed to the same reason mentioned previously since the crystal size has grown by the increased cerium oxide doping ratio[31] .

Figure 11 to 14 show plot diagrams of extinction coefficient, refractive index, and real and imaginary parts of dielectric constant. It is clear that the addition of cerium oxide to tin oxide increased the transmittance and hence reduced the values of the optical constants (n, k, ε_r, and ε_i). All have the highest value at 7% doping concentration, as shown in Table 4.
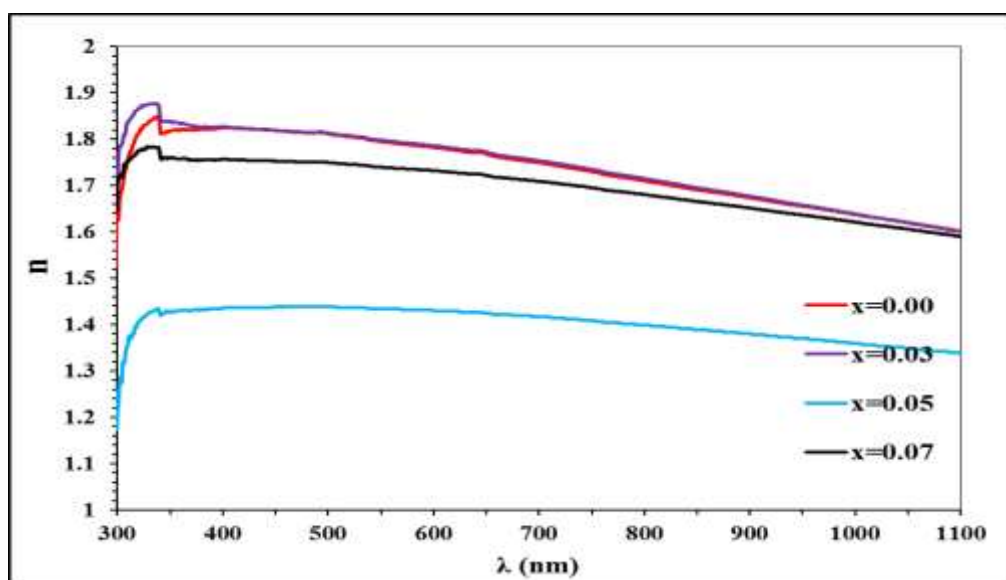
Figure 11: **R**efractive index as a function of wavelength for pure SnO_2 and CeO_2 doped SnO_2 thin films.
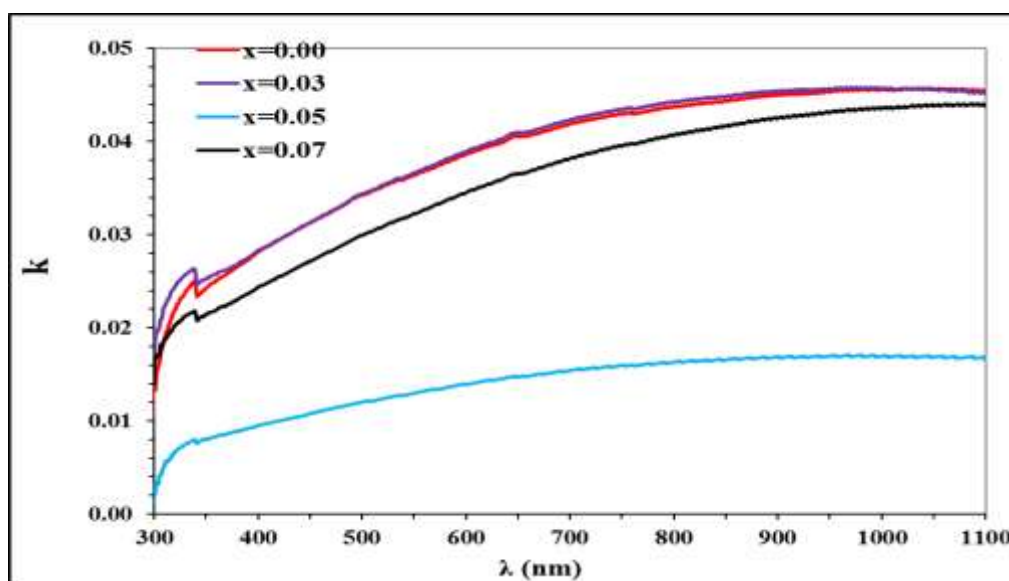
Figure 12: Extinction coefficient as a function of wavelength for pure SnO_2 andCeO_2 doped SnO_2 thin films.
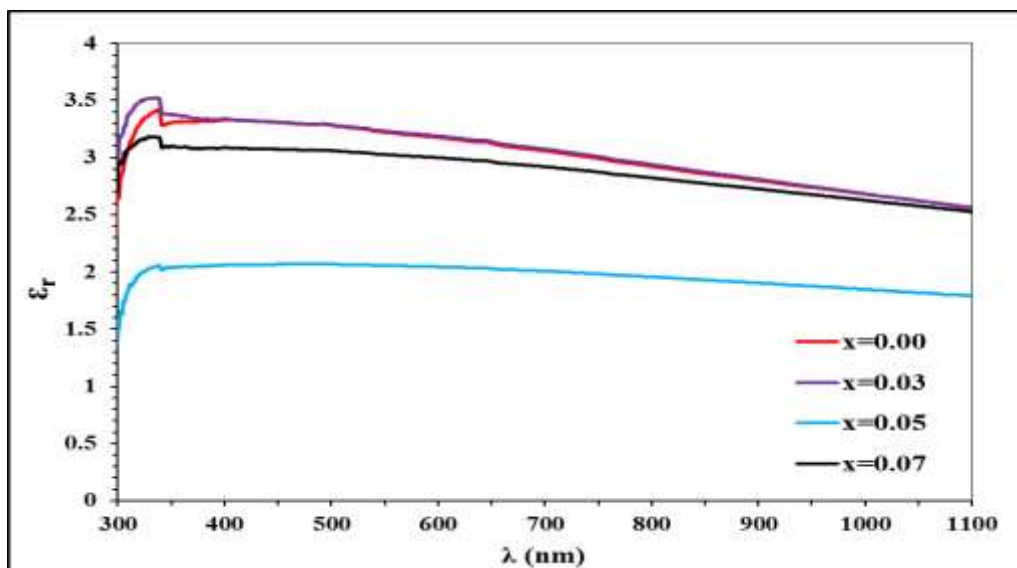
Figure 13: Real part of dielectric constant as a function of wavelength for pure SnO_2 andCeO_2 doped SnO_2 thin films.
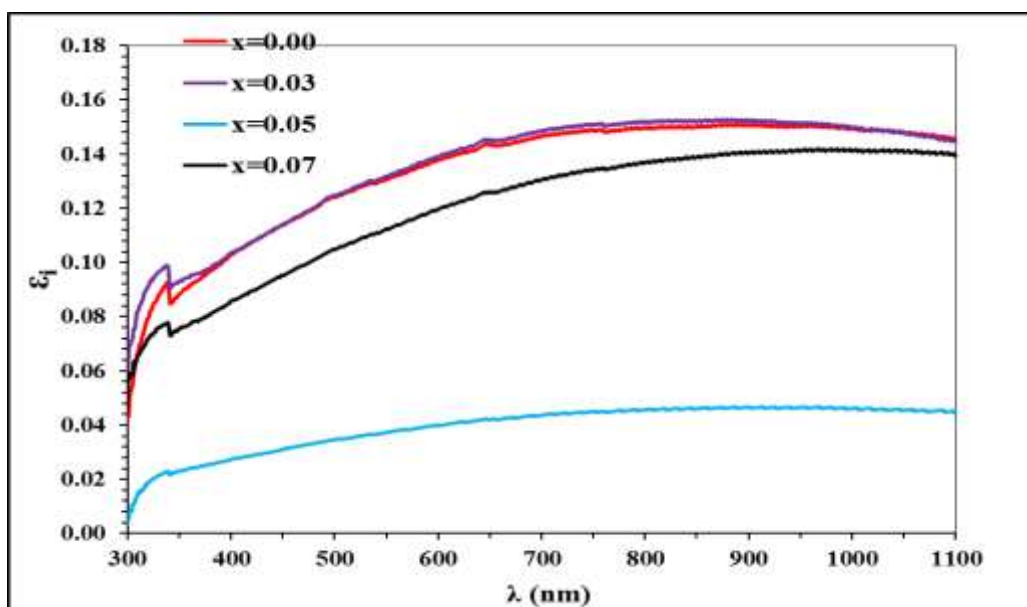
Figure 14: Imaginary part of dielectric constant as a function of wavelength for pure SnO_2 andCeO_2 doped SnO_2

Table 4: the transmittance, absorption coefficient, optical properties and optical energy gap of $(SnO_2):(CeO_2)$ thin films that have been prepared through using the PLD approach.

Samples	T%	α (cm^{-1})	k	n	ε_r	ε_i	Eg (eV)
SnO_2	84.67	8320	0.036	1.796	3.223	0.131	3.60
SnO_2:3%CeO_2	84.58	8377	0.037	1.799	3.235	0.132	3.60
SnO_2:5%CeO_2	94.24	2965	0.013	1.434	2.057	0.037	3.58
SnO_2:7%CeO_2	86.30	7370	0.032	1.741	3.029	0.112	3.55

Conclusions:
   From the study, the following can be concluded:
1-All the prepared thin films had polycrystalline structure.

2- Doping with gallium oxide led to a significant enhancement of the degree of crystallinity while doping with cerium oxide had unnoticeable change of crystal structure.

3- Doping with gallium oxide and cerium oxide up 5% made the prepared samples more opaque and more transparent respectively and then the opposite take place.

4- Doping with gallium oxide led to non- regular change of optical energy gap while doping with cerium oxide led to a progressive reduction of the energy gap.

References

[1] R.M. Pasquarelli, D.S. Ginley, R. O'Hayre, "Solution Processing of Transparent Conductor: from Flask to Film," *Chem. Soc. Rev*, vol. 40, no. 11, pp. 5406, 2011.

[2] H. Hosono, "Recent Progress in Transparent Oxide Semiconductors: Materials and Device Application," *Thin Solid Films*, vol.515, no. 15, pp. 6000, 2007

[3] M. Batzill, U. Diebold, "The surface and materials science of tin oxide," *Prog. Surf. Sci.* vol. 79, no. 2-4, pp. 47-154, 2005

[4] M.H. Phillips, Y. Li, Z. Bi, B. Zhang, "Reactive pulsed laser deposition and laser induced crystallization of SnO_2 transparent conducting thin films," *Appl. Phys. A*, vol. 63, pp. 347-351, 1996

[5] C.L. Hsu, Y.C. Lu, "Fabrication of transparent ultraviolet detector by using n-type Ga_2O_3 and Ga-doped SnO_2 coreshell nanowires," *Nanoscale,* vol. 4, no. 18, pp. 5710-5717, 2012

[6] H. M.. Kim,S. H. Choi, H. J. Jeong, J. H. Lee, J. Kim, and J. s. Park, " Highly dense and stable p-type Thin film transistor based on atomic layer deposition SnO fabricated by two-step crystallization," *ACS Appl. Mater Interfaces*, vol, 13, no. 26, pp. 30818-30825, 2021

[7] V. P. Meshalkin, and A. V. Belyakov, " Methods Used for the Compaction and Molding of Ceramic Matrix Composites Reinforced with Carbon Nanotubes". *Seong Solid State Lett*. vol. 8, no. 8, pp. 1004, 2020

[8] R. E. Presley, C. L. Munsee, C. H. Park, D. Hong, J. F. Wager, D.A. Keszler,"Tin oxide transpanter thin film transistors ," . *Appl. Phys.D: Applied Physics*, vol. 37, no. 20, p. 2810, 2004

[9] C. Tsay, c. W. Wu, M. Lei. F. S Chen, C. K. Lin, " Microstructural and optical properties of Ga-doped ZnO semiconductor thin films prepared by sol–gel process", *Thin Solid Films*, vol. 519, no. 5, p. 1516-1520, 2010.

[10] A. K. Singh, A. Janotti, M. Scheffler, C.G. van de Walle, "Sources of Electrical Conductivity in SiO_2 ," *Physical Review Letters*, vol. 101, no. 5, p. 055502, 2008.

[11] J. Du. Z.G. Ji, Acta Phys. Sin. vol.56, pp. 2388, 2007

[12] S. S. Wn. H. Q. Cao, S. F. Yin, X. W. Liu, X. R. Zhang, J.C. Chem, "Synthesis Comparative Characterization and photocatalytic application of SnO_2". vol. 113, pp. 17893, 2009

[13] C. Wang, C. Shao, X. Zhang, Y. Liu," SnO_2 Nanostructures-TiO_2 Nanofibers Heterostructures: Controlled Fabrication and High Photocatalytic Properties" *Inorg. Chem.*, vol.48, pp.7261, 2009

[14] N. Wang, J. Xu, L. Guan, " Prospects of Nanobiomaterials for Biosensing" *Mater. Res. Bull*. vol.46, pp. 2378, 2011

[15] D. Liu, T. Liu, H. Zhang, Lv Chengling, L.C, Zeng, W. Zhang, "Gas sensing mechanism and properties of Ce-doped SnO, sensors for volatile organic compounds" *Mater. Sci, Semicond. Processing*, vol. 15, no. 4, pp. 438-444, 2012

[16] N. Yan, Z. Zhu, J. Zhang, Z . Zhao, and Q. Liu, " Preparation and properties of Ce doped TiO_2 photocatalyst," *Mater. Res. Bulletin*, vol.47, no. 8, pp. 1869-1873, 2012.

[17] X. Lian, Y. Li, X. Tong, Y. Zou, X. Liu, D. An, and Q. Wang, " Synthesis of Ce-doped SevO; nanoparticles and their acetone gas sensing properties," *Applied Surface Science*, vol. 407, pp. 447-455, 2017

[18] S. Chen, X. Zhao, H. Xie, J. Liu, L. Duan, X. Ba,and J. Zhao, "Photoluminescence of undoped and Ce-doped SnO_2 thin films deposited by sol-gel-dip-coating method," *Appl.Surf. Sci.*, vol. 258, no. 7, pp. 3255-3259, 2012

[19] B. L. Zhu, X. Zhao, W.C. Hu, T. Li, J. Wu, Z. H. Gan, J. Liu, D. Zeng, and C.S Xie, "Structural, electrical, and optically d properties of F-doped SnO or SnO_2 films prepared by RF reactive magnetron sputtering at different substrate temperatures and O_2 fluxes," *Applied physics*, vol. 719 ,pp. 429-437, 2017

[20] R. T. Jacob, J. Thomas, R. George, M. Kumaran, Govardhan, "Comparative study on ammonia sensing properties of SnO₂ nano composites fabricated via electropinning and sol gel processes," *International Journal of Research in Engineering and Technology*, vol. 3, no. 5, pp. 599-605, 2014.

[21] A. Goswami, *"Thin Film Fundamental". New Age International (P) Limited publishers, New Delhi*, 1996.

[22] S N. Vidhya, O. N. Balasundaram, M. Chandramohan, "Structural and optical investigations of gallium doped tin oxide thin films prepared by spray pyrolysis," *journal of Saudi Chemical Society*, vol. 20, no. 6, pp.703-710, 2016

[23] F. Finanda, Damisih, Hong Chan Ma and Hee Young Lee, "Characteristics of p-type gallium tin oxide (GTO) thin films prepared by RF magnetron sputtering", *Journal of Ceramic Processing Research*, vol. 13, pp. s181-s185, (2012)

[24] S. S. Mahmood, and B. A. Hasan, "Characterization of (SnO2)1-x(TiO2:CuO)x films as NH3 gas sensor," *Iraqi Journal of Physics*, vol. 16, no. 39, pp. 71-80, 2018

[25] S. S. Mahmood, B. A. Hasan, "Effect of Dopant Concentration on the Structural, Optical and Sensing Properties of (SnO2)1-x(TiO2:CuO)x Sprayed Films," *Baghdad Science Journal*, vol. 16, no. 2, pp. 361-369, 2019.

[26] R. C. Deus, R. A. C. Amoresi, P. M. Desimone, F. Schipani, L. S. R. Rocha, M. A. Ponce, A.Z. Simoes, E. Longo, "Electrical behavior of cerium dioxide films exposed to different gases atmospheres," *Ceramic international*, vol.42, pp. 15023-15029, 2016

[27] C. A. Vincent, "The nature of semi conductivity in polycrystalline tin oxide," *Journal of The Electrochemical Society*, vol. 119, pp.515-518, 1972.

[28] K. L. Chopra, S. Major, and D. K. Pandya, "Transparent conductors—a status review," *Thin Solid Films*, vol. 102, no. 1, pp. 1-46, 1983.

[29] Z. Chen, J. Lai, C. H. Shek, C.H. and H. Chen, "Synthesis and structural characterization of rutile SnO2 nanocrystals," *Journal of materials research*, vol. 18, no. 06, pp. 1289-1292, 2003

[30] S.M.N. Vidhya, O. N. Balasundaram, M. Chandramohan, "A Brief Review on the Polymer thin Film Solar Cells," *journal of Saudi Arabia*, vol. 20, pp. 703710, 2016

[31] J.Tauc(Ed.) , *"amorphous and liquid semiconductors'. Springer New York, NK* , 1974.